Negative-ion photodetachment in an electric field

Hin-Yiu Wong, A. R. P. Rau, and Chris H. Greene
Department of Physics, Louisiana State University, Baton Rouge, Louisiana 70803
(Received 24 August 1987)

A multichannel study of the photodetachment of a negative ion such as S^- in the presence of a constant electric field is presented. The analysis is carried out as a series of frame transformations for the outgoing photoelectron. An earlier analysis in the absence of the external field is now augmented by the further transformations from spherical to cylindrical symmetry that are required. The interplay between the various thresholds due to fine structure in the negative ion and residual atom and the effects of the external field are analytically treated. The net effect is to eliminate the thresholds, to induce modulations in the detachment cross section, and to introduce field-assisted-tunneling contributions to the photodetachment. Numerical illustrations are provided. Our treatment closely parallels similar treatments of photoionization of neutral atoms in an electric field and of photodetachment in a magnetic field.

I. INTRODUCTION

We consider the photodetachment of a negative ion in the presence of an external electric field. There has been considerable experimental and theoretical activity in recent years in the allied problems of photoionization of neutral atoms in external electric or magnetic fields.[1,2] Likewise, some experimental data is available on the photodetachment of a negative ion in a magnetic field.[3] Although similar experiments with comparable resolution have not yet been carried out on photodetachment in an electric field,[4] such experiments are feasible. In fact, we hope that our analysis and some of the features revealed by it may prompt such an experimental study. In any case, the motivation for our study is that it complements other theoretical analyses of photoionization in an electric field[5] and photodetachment in a magnetic field.[6] All these share the common element of competing symmetries that prevail for the motion of the electron at small and large radial distances, with the external field in particular playing a role only at large r.

The effect of the external field is entirely negligible for the small-r motion and this feature is exploited to cast all cross-section expressions in a simple, factorized form. The zero-field cross section is multiplied by a "modulating factor," into which is absorbed the entire influence of the external field. This factor reduces to unity when the field strength goes to zero. The modulating factor is derived as an aspect of a "frame transformation"[5,7] between the descriptions relevant to small and large r. The feature which distinguishes these external-field frame transformations from other frame transformations between orthogonal bases in spectroscopy and scattering is that the transformations are now nonorthogonal. Nevertheless, as pointed out by the pioneering study of Fano[8] and of Harmin[5] for photoionization in an electric field, the transformation and the modulating factor it leads to can be worked out explicitly when the large-r motion in the long-range fields is exactly solvable in some suitable system of coordinates. Their work rested on the fact that motion in the combined Coulomb and electric field potentials has an analytical solution in parabolic coordinates.[9] Our paper, and the companion paper[6] by one of us, consider two other instances where such solutions are available, namely, when the long-range potential is due to an electric field alone or due to a magnetic field alone. Together, these studies serve to illustrate both the common elements of such analyses and the specific differences that each specific potential brings. We hope that taken together these studies will show how to use the theory of nonorthogonal frame transformations. Finally, we note that what still stands in the way of extending this analysis to the more challenging, and at the same time more studied (experimentally and through numerical calculations), problem of photoionization in a magnetic field is that no set of coordinates is available for describing the motion of an electron at large r in combined Coulomb and diamagnetic potentials.

For concreteness, we analyze a specific negative ion, namely, S^- (or its analogs, O^- and Se^-). Our choice is made because there exists already a detailed theory of multichannel photodetachment in this system in the absence of an external field.[10] This theory has been described in terms of frame transformations (albeit orthogonal ones) between small and large r. The description at small r and part of the transformation to large r are, therefore, already available. It remains then for us to develop the added transformation introduced by the external field to have a full treatment of the problem. We also note that it is precisely in the S^- negative ion that experimental data is available on photodetachment without an external field[11] and with a static, magnetic field.[3]

As in the previous study[10] of S^- photodetachment in zero field, we restrict ourselves to the region around the threshold for this process

$$S^-(^2P_{3/2,1/2})+h\nu\rightarrow S(^3P_{2,1,0})+e\,(l=0)\ . \qquad (1.1)$$

Six different fine-structure channels are available, depending on the states of the negative ion and the neutral atom.

We derive expressions for the cross section as a function of photon energy and as a function of the electric field strength F. These expressions differ in two ways from the $F=0$ results available in the literature.[10] First, the old cross sections are modulated by an F-dependent factor; second, there is, of course, no photodetachment threshold since all channels are automatically open in the presence of the electric field. Even when this energy falls short of the smallest separation between S^- and S states (specifically, the $^2P_{3/2}$ and $^3P_2$ states), electrons can still be ejected because of energy derived from the external field F. We will show how our expression for the cross section becomes proportional far below the threshold photon energy to the probability of field ionization by way of tunneling[12] through the linear Stark potential Fz. We will assume a static field in the z direction and use atomic units throughout.

A. Identification of appropriate coordinates

The relevant potential for a photoelectron in an electric field is

$$V(r)=V_s(r)+Fz \ , \tag{1.2}$$

where $V_s(r)$ is the short-range interaction with the neutral atomic core. We will parametrize its effect most simply by zero-field quantum defects, or the equivalent scattering lengths. Since $F \ll 1$ for almost all fields of interest (1 a.u. of electric field $=5.1\times 10^9$ V/cm), the term in F is entirely negligible at small distances. This is a key to our analysis and to all similar analyses of external electric- and magnetic- (diamagnetic potential) field effects. On the other hand, at large distances, the multiplicative dependence on the radial extent (z in the Stark problem, x^2+y^2 in the diamagnetic) makes these field dependent terms the dominant ones. [In photoionization of neutral atoms, the long-range Coulomb tail needs to be superimposed, but for the negative-ion problems that concern us, the second term in (1) is the sole long-range potential.] This initial assessment of (1) points to the suitable descriptions for the small- and large-r parts of the problem. Spherical polar coordinates are the obvious choice for the former, and this choice is common to all such analyses. At large r, however, we may use in the present problem Cartesian, cylindrical, or parabolic coordinates because the Schrödinger equation for the potential Fz separates in all these systems. We elect to work with cylindrical coordinates for two reasons. First, it is the natural choice for the companion analysis[6] of photodetachment in a magnetic field. Second, we can proceed to the final steps through simple, analytical expressions whereas the choice of parabolic coordinates is more clumsy in this regard (note that this is the necessary choice when a Coulomb tail is superimposed on Fz). Exploratory calculations in parabolic coordinates appear to give equivalent results.

B. Different ranges of motion

The short range $V_s(r)$ in (1) extends over a few a.u. We will call this region I for the photoelectron's motion. Outside this region, since the term in F only becomes significant for distances exceeding several hundred a.u., it is useful to subdivide further into two regions. An intermediate region II, still described in spherical coordinates and with angular momentum $l(=0)$ a good quantum number, stretches to $\simeq 10^3$ a.u. It is only beyond this that we are in region III, which then stretches to asymptotic infinity, and where the Fz term and its cylindrical symmetry prevail. Each passage between regions is accompanied by a frame transformation between the descriptions of the wave function that are appropriate to each region.

The passage from region I to region II is as in the $F=0$ problem. The same (spherical) coordinate system applies in both these regions so that the passage consists only of an orthogonal transformation of the angular and spin parts of the wave function and a rewriting of the radial wave function from the form appropriate to small r to that for large r. The orthogonal transformation is[10] an $LS \rightarrow jj$ recoupling because these are the respective coupling schemes applicable to region I (when the photoelectron is strongly coupled to the core) and region II (when the photoelectron is separated from the core so that the spin and orbital angular momentum of each are first coupled among themselves). For the low energies near threshold that are of concern to us, the small-r radial wave function (with $l=0$) in region I will be described by a single set of parameters, a_d and a_q, the scattering lengths for the doublet and quartet states of the $[e(^2s)+S(^3P)]$ system. (Two more parameters, the effective ranges, may be added if more accuracy or a broader energy coverage is desired.) The total angular momentum J remains a good quantum number throughout regions I and II.

C. Scheme of the analysis

In the earlier work[10] at $F=0$, only one simple step remained to connect the region II wave functions to the expressions for cross sections. This was to apply boundary conditions ("ingoing wave") at infinity that are appropriate to the photoelectron's emergence in one or the other of the alternative channels characterized by the j value of the residual ^3P atom that is left behind. At the same time, since experiments monitor the electron or the atom and not the total angular momentum J, one had to decouple the j values of the two fragments (this involved a Clebsch-Gordan coefficient) and superimpose amplitudes for alternative J values that contribute to an observed cross section. In the current paper, more novel and nontrivial elements enter into the passage from region II to III. With the breaking of spherical symmetry by the electric field, J is not a good quantum number. Only the projection M_J retains status as a conserved quantity. A Clebsch-Gordan coefficient and superposition of J values is, therefore, again one element of the frame transformation between these regions. In addition, there is the recasting of the full wave function from its spherical description in region II to the cylindrical one appropriate to region III. Apart from the common coordinate ϕ, the azimuthal angle conjugate to M_J, this is

effectively a two-dimensional transformation $(r,\theta)\rightarrow(\rho, z)$. Following Harmin's similar transformation from spherical to parabolic bases,[5] the initial step is to make a local coordinate transformation in region I (where F is still negligible) between wave functions of a free particle from spherical to cylindrical bases. At this point, as the bases are orthogonal, so is the transformation $U^{F=0}$. Next, the fact that the wave functions of the asymptotic scattering states in region III (which are dependent on F) must be proportional at smaller distances to the region II cylindrical wave functions is exploited to get the nonorthogonal transformation U^F that recasts the region II functions in terms of those for region III. This is the key result of our analysis because the modulating factor in the cross sections is essentially the square of U^F.

The arrangement of this paper is as follows. In Sec. II we describe the wave functions in regions I and II and the frame transformation $U^{(J)}_{jS}$ between them. The reaction matrix $K^{(J)}_{jj'}$ that is diagonal in J and connects alternative states j and j' of the residual atom is defined. This section also presents the subsequent passage to a reaction matrix between asymptotic states i in region III which are characterized by M_J. The Clebsch-Gordan coefficient $W^{(M_J)}_{iJ}$, which is the orthogonal piece of the frame transformation for this part of the analysis, is defined as well as the reaction matrix $K^{(M_J)}_{ii'}$, and its eigenvalues and eigenvectors. Section III deals with the local coordinate transformation between spherical and cylindrical bases, the derivation of U^F, and the modulating factor H^F. In Sec. IV explicit expressions for the cross section $\sigma^F(j)$ into the different j states of the neutral atom residue are derived. Finally, Sec. V gives numerical results in graphical form for H^F and σ^F, showing the modulations induced by the electric field. The discussion also includes an analytical demonstration that for energies below the zero-field photodetachment threshold, σ^F goes over into the result for field ionization of electrons from a negative ion. Three appendices elaborate on alternative normalization schemes for small-r radial functions, the derivation of U^F, and the evaluation of H^F.

II. FRAME TRANSFORMATION FROM REGION I ($\lesssim 10a_0$) TO REGION II ($10-10^3a_0$)

This section is in the main a paraphase of the analysis of photodetachment in zero field.

A. Wave function at small r

The initial negative ion has an electron distribution confined to a few a.u. The absorption of the photon puts enough energy to create a complex, $(e+\mathrm{S})$, which subsequently fragments and the electron and atom separate to infinity. In viewing this complex initially at small r (region I), the electron is highly coupled to the remaining electrons in the neutral atom and an appropriate description of the complex is provided by LS coupling. For our near-threshold analysis (dominated by $l=0$ for the electron), the only value of L that is of interest is $L=1$ as in the ground state (^3P) of sulfur. Two alternative values, $S=\frac{1}{2}$ and $\frac{3}{2}$, are, however, involved for the total spin of the complex. Further, let J and M_J be the total angular momentum and its azimuthal projection of the $(e+\mathrm{S})$ complex. Representing the angular and spin wave function in LS coupling (together with the radial function for the electrons in the sulfur atom) by $X^S_{JM_J}$, the full wave function of the complex in region I can be written as

$$X^S_{JM_J}(r-a_s)(2/\pi)^{1/2} . \tag{2.1}$$

The radial wave function for the $l=0$ electron has been written in its simplest form in terms of the scattering length (doublet and quartet scattering lengths) and has been normalized independently of the asymptotic energy of the electron. This is appropriate for region I where the asymptotic energy is an irrelevant parameter, being dwarfed by the strong potentials that prevail in this region. This choice and the numerical factor in (2.1) are in conformity with standard frame transformation theory[7] where the state described by (2.1) is denoted $|\alpha^0\rangle$. We defer to Appendix A the minor modifications necessary in all subsequent expressions were we to use energy-normalized states $|\alpha\rangle$ which are related to (2.1) through

$$|\alpha\rangle = k^{1/2}|\alpha^0\rangle , \tag{2.2}$$

where k is the wave number, $k=(2\mu E/\hbar^2)^{1/2}$.

B. Wave function at large r

When the electron separates from the sulfur atom and passes into region II, jj coupling is appropriate and the channels $|j\rangle$ in this domain are characterized as

$$|(L^aS^a)j,k_j(l_es_e)j_e,JM_J\rangle . \tag{2.3}$$

Superscripts a refer to the atom, subscripts e to the electron, and J is the total angular momentum of the atom. Since the energy of the outgoing electron depends on the state j of the residual atom, its wave number also depends on j and is so denoted. J and M_J are once again the total angular momentum quantum numbers of the system.

Denoting the wave function of the atom, together with the angular and spin functions of the photoelectron in jj coupling by $\phi^j_{JM_J}$, the total wave function of the complex in region II is

$$\psi_j = \phi^j_{JM_J}f_j(r) - \sum_{j'} K^{(J)}_{jj'}\phi^{j'}_{JM_J}g_{j'}(r) . \tag{2.4}$$

A superposition of regular $f(r)$ and irregular $g(r)$ radial functions reflects the effect of the short-range core effects on the wave function in this region. K, the reaction matrix, is diagonal in J. Our choice for the radial functions are the energy-normalized free-particle functions[13] for $l=0$,

$$f_j(r) = (2/\pi k_j)^{1/2}\sin k_j r , \tag{2.5a}$$

$$g_j(r) = -(2/\pi k_j)^{1/2}\cos k_j r . \tag{2.5b}$$

C. Definition of the K matrix

To obtain an expression for the K matrix, (2.4) has to be matched to (2.1). All but the radial part involve the

orthogonal $LS \rightarrow jj$ transformation,[14]

$$X^S_{JM_j} = \sum_j \phi^j_{JM_j} U^{(J)}_{jS} , \tag{2.6}$$

whereas the radial connection follows from matching the small-r forms of (2.5) to (2.1). We have

$$K^{(J)}_{jj'} = -\sum_S U^{(J)}_{jS} k_j^{1/2} a_S k_{j'}^{1/2} U^{(J)}_{j'S} . \tag{2.7}$$

The frame transformation matrix U is given for $U^{(3/2)}_{jS}$ and $U^{(1/2)}_{jS}$, respectively, by[10]

j \ S	$\frac{3}{2}$	$\frac{1}{2}$
1	$\sqrt{\frac{5}{6}}$	$-\sqrt{\frac{1}{6}}$
2	$\sqrt{\frac{1}{6}}$	$\sqrt{\frac{5}{6}}$

j \ S	$\frac{3}{2}$	$\frac{1}{2}$
0	$\sqrt{\frac{2}{3}}$	$-\sqrt{\frac{1}{3}}$
1	$\sqrt{\frac{1}{3}}$	$\sqrt{\frac{2}{3}}$

(2.8)

The allowed values of J following photoabsorption are $J=\frac{1}{2}$ and $\frac{3}{2}$ regardless of whether the initial state of S^- is $^2P_{1/2}$ or $^2P_{3/2}$. A third value, $J=\frac{5}{2}$, is allowed by dipole selection rules upon starting from the $\frac{3}{2}$ state of the negative ion but is only compatible with the quartet state of the $(e+S)$ $L=1$ complex. Since the spin of the complex is substantially unchanged upon photoabsorption (spin-orbit coupling being small in a few-electron system such as this), we drop $J=\frac{5}{2}$ from further consideration as negligible.

D. Imposition of boundary conditions on the wave function

In general, two different j values contribute to each J. Thus, for any J, the full wave function is a superposition of functions (2.4); for instance, for $J=\frac{3}{2}$,

$$\psi = c_1\psi_1 + c_2\psi_2 . \tag{2.9}$$

When both j channels are open, i.e., k_1 and k_2 are real, $\psi_{1,2}$ take the form

$$\psi_1 = \phi^1_{3/2} f_1(r) - \phi^1_{3/2} g_1(r) K^{(3/2)}_{11} - \phi^2_{3/2} g_2(r) K^{(3/2)}_{21} , \tag{2.10a}$$

$$\psi_2 = \phi^2_{3/2} f_2(r) - \phi^1_{3/2} g_1(r) K^{(3/2)}_{12} - \phi^2_{3/2} g_2(r) K^{(3/2)}_{22} . \tag{2.10b}$$

(For convenience of display, the subscript M_J on the ϕ's has been dropped.)

If the photoelectron escapes in, say, channel $j=2$, the coefficient of the outgoing wave in (2.9) in the other channel ($j=1$) must be set equal to zero and, at the same time, for purposes of energy normalization the coefficient in the channel $j=2$ must be $(\frac{1}{2}i)(2/\pi k_2)^{1/2}$. These boundary conditions require

$$c_1 = -\frac{iK^{(3/2)}_{12}}{1+iK^{(3/2)}_{11}} c_2 , \tag{2.11a}$$

$$c_2 = \frac{1+iK^{(3/2)}_{11}}{[1-K^{(3/2)}_{11}K^{(3/2)}_{22}+(K^{(3/2)}_{12})^2]+i(K^{(3/2)}_{11}+K^{(3/2)}_{22})} . \tag{2.11b}$$

Likewise, if escape into the channel $j=1$ is of interest, the subscripts in (2.11) are interchanged.

On the other hand, if only one of the channels is open as, for instance, just above the threshold for photoabsorption by $^2P_{3/2}$, when $j=1$ is still closed and only $j=2$ open, we have to set $k_1=-i\kappa_1$ and "eliminate" this channel by forcing its wave function to vanish (exponentially) at infinity.[15] This will leave behind for ψ in (2.9) only contributions from $j=2$,

$$\psi = c\phi^2_{3/2}[f_2(r) - g_2(r)\tan\delta^{(3/2)}] , \tag{2.12}$$

and the 2×2 reaction matrix is replaced by the simple phase

$$\tan\delta^{(3/2)} = K^{(3/2)}_{22} - \frac{i(K^{(3/2)}_{12})^2}{1+iK^{(3/2)}_{11}} . \tag{2.13}$$

Note that (2.13) is explicitly real in spite of the appearance of i in two places; this imaginary element is compensated by the imaginary elements introduced in (2.7) through k_1. The normalization constant c in (2.12) so that ψ is energy normalized, as are f_2 and g_2, is given by

$$c = (1+\tan^2\delta^{(3/2)})^{-1/2} . \tag{2.14}$$

Similar expressions obtain for $J=\frac{1}{2}$ where $j=0,1$ play the role of $j=1,2$ in the above expressions. As an example, when $j=1$ is open but $j=0$ closed, the reaction matrix is replaced by the single real phase, the analog of (2.13),

$$\tan\delta^{(1/2)} = K^{(1/2)}_{11} - \frac{i(K^{(1/2)}_{10})^2}{1+iK^{(1/2)}_{00}} . \tag{2.15}$$

Finally, regardless of the number of channels open, it is useful to extract the large-r form of the collision eigenchannel wave functions,

$$\psi_\rho \rightarrow \sum_{j \text{ open}} \phi^j_J T_{j\rho}[f_j(r)\cos\delta_\rho - g_j(r)\sin\delta_\rho], \quad r\rightarrow\infty \tag{2.16}$$

in which any closed-channel components which might be present are exponentially small at large r. For the situations involving only one open channel, the one by one matrix T is, of course, unity and the collision eigenphase-shifts are given by either (2.13) or (2.15). At higher energies for any J, both contributing channels j are open and the eigen-phase-shifts $\delta^{(J)}_\rho$ are the arctangents of the eigenvalues of the (at most 2×2) reaction matrix (2.7). Successive columns of the orthogonal matrix $T_{j\rho}$ are simply the corresponding eigenvectors of this reaction matrix. These eigenparameters succinctly describe the wave function of the photoelectron as it escapes spherically from the residual atom, prior to experiencing the external field.

III. TRANSFORMATION FROM SPHERICAL TO CYLINDRICAL SYMMETRY

The primary feature of photodetachment in an electric field is that the photoelectron passes from a domain of spherical to one of cylindrical symmetry as it goes from

region II to III. In this section the appropriate transformation factor will be derived so that the wave function ψ of the final-state eigenchannels can be adapted to the (cylindrical) symmetry that pertains at infinity. This will then give through the density of states $D_{\rho\rho'}=[\langle\psi\,|\,\psi\rangle^{-1}]_{\rho\rho'}$ the modulating factor that expresses the effect of the electric field on the cross sections.

A. Transformation at $F=0$

Region II is the region of overlap between both symmetries. We will first derive the orthogonal transformation that connects free-particle wave functions in the two descriptions. The regular, energy-normalized spherical solutions for a free electron are[13]

$$F_{lm}(\mathbf{r})=(2\pi)^{-1/2}e^{im\phi}N_{lm}P_l^m(\cos\theta)r^{1/2}J_{l+1/2}(kr)\ , \tag{3.1}$$

where

$$N_{lm}=(-1)^{(|m|+m)/2}i^l\left[\frac{2l+1}{2}\frac{(l-|m|)!}{(l+|m|)!}\right]^{1/2}\ . \tag{3.2}$$

For $l=0$, this coincides with (2.5a) except that the angular part of the wave function [which is $(4\pi)^{-1/2}$ for $l=0$] is also included in (3.1). In expressing spherical and cylindrical solutions in terms of one another, we need in general all values of l, although in the final expressions for cross sections only the coefficients involving $l=0$ will appear, reflecting that the initial "feed" into region II is only in the s wave.

On the other hand, the regular energy-normalized cylindrical solutions are

$$\psi_{qm}(\mathbf{r})=\frac{e^{im\phi}}{(2\pi)^{1/2}}J_m[(k^2-q^2)^{1/2}\rho]\times(\pi q)^{-1/2}\times\begin{cases}\cos qz, & \Pi_z=+1\\ \sin qz, & \Pi_z=-1\ .\end{cases} \tag{3.3}$$

The two different forms are for even and odd "z parity." Since the reflection $z\to -z$ corresponds to $\theta\to\pi-\theta$, clearly $\Pi_z=(-)^{l+m}$, so that the expansion of $\psi_{qm}(\mathbf{r})$ in terms of $F_{lm}(\mathbf{r})$ will involve either only even or only odd terms in $l+m$. The index q in (3.3) is the wave number for the z motion; that is, we have apportioned the total energy $(\frac{1}{2})k^2$ into $(\frac{1}{2})q^2$ for the z motion and $(\frac{1}{2})(k^2-q^2)$ for the ρ motion. Note also that in expanding (3.1) and (3.3) in terms of each other, for a free particle we expect q to run from 0 to k; however, for later applications when an external field F is present with its potential Fz which runs to $-\infty$, q^2 can also range over negative values.

The expansion coefficients in

$$\psi_{qm}(\mathbf{r})=\sum_l U_{ql}^{F=0}F_{lm}(\mathbf{r}) \tag{3.4}$$

can be obtained in several ways. Relegating alternative procedures, as well as the general expression for all l, to Appendix B, perhaps the simplest step to obtain the $l=0$ coefficient that is of interest to us is to examine both sides of (3.4) for $\mathbf{r}\to 0$ (that is, $\rho\simeq z\simeq r\simeq 0$). As expected, for $l=0$ only $\Pi_z=1$ is relevant, and simple inspection gives

$$U_{q0}^{F=0}=(kq)^{-1/2}\ . \tag{3.5}$$

The simple derivation of the transformation (3.4) is valid at least locally (at reasonably small r) and that will suffice for our purposes when we later extend to $F\neq 0$. The generalization of (3.4) to arbitrary lm is given in Ref. 6. Note also in this context that the result in (3.5) also pertains if q were to be imaginary, $q=iq'$. The result is, of course, not meaningful for all $\mathbf{r}$ and, in particular, for large distances, but $\cos iq'z$ remains bounded so long as $q'z$ is small. Finally, again for later extension to $F\neq 0$ we need the analytic continuation to negative energy, $k^2=-\kappa^2<0$. The $l=0$ (real) energy-normalized function is chosen as

$$F_{00}(\mathbf{r})=(2\pi^2\kappa)^{-1/2}\frac{\sinh\kappa r}{r}\ . \tag{3.6}$$

Correspondingly, with $q^2<-\kappa^2$, which is necessary so that the kinetic energy in ρ remains positive (the argument of J_0 below is real) we have

$$\psi_{q0}(\mathbf{r})=(2\pi^2 q)^{-1/2}J_0[i(\kappa^2+q^2)^{1/2}\rho]\cos qz\ , \tag{3.7}$$

The passage between them, again valid at least at small r and obtained as before by inspection, is

$$U_{q0}^{F=0}=(\kappa q)^{-1/2}\ . \tag{3.8}$$

B. Transformation at finite field

In the presence of a static electric field, the exact energy-normalized cylindrical solution for a free electron of energy $(\frac{1}{2})k^2$, with again $(\frac{1}{2})q^2$ apportioned to the z motion, is

$$\psi_{qm}^F(\mathbf{r})=(2\pi)^{-1/2}e^{im\phi}J_m[(k^2-q^2)^{1/2}\rho]\times(4/F)^{1/6}\mathcal{A}[(2F)^{1/3}(z-q^2/2F)]\ , \tag{3.9}$$

where $\mathcal{A}$ is the Airy function;[16] q^2 can now range from $-\infty$ to k^2. The crucial step is now the recognition that in computing a transition dipole matrix element $\langle\psi_{qm}^F\,|\,z\,|\,\Psi_0\rangle$ for photoabsorption, where Ψ_0 is the ground-state wave function of S^-, the relevant region is at small r only (region I) which is where Ψ_0 is appreciable. Therefore, apart from normalization factors, F does not affect the structure of the matrix element itself. We can reexpress ψ_{qm}^F at small distances in terms of the $F=0$ functions ψ_{qm} in (3.3),

$$\psi_{qm}^F(\mathbf{r})=A_+\psi_{qm}^+(\mathbf{r})+A_-\psi_{qm}^-(\mathbf{r})\ , \tag{3.10}$$

where the superscripts on ψ on the right denote the value of Π_z. Note, of course, that both z parities are involved in representing the mixed-parity object in (3.9), this parity being no longer a good quantum number when $F\neq 0$. The coefficients $A_\pm$ are obtained by setting $z\simeq 0$ because the emphasis in this expansion of the $F\neq 0$ function in terms of the $F=0$ ones is that it need only be valid at small distances. We have

$$A_+=(\pi q)^{1/2}(4/F)^{1/6}\mathcal{A}[-q^2/(2F)^{2/3}]\ , \tag{3.11a}$$

$$A_-=(\pi/q)^{1/2}2^{2/3}F^{1/6}\mathcal{A}'[-q^2/(2F)^{2/3}]\ . \tag{3.11b}$$

On combining with (3.4), we have the transformation between cylindrical and spherical symmetry valid for $F\neq 0$

$$\psi^F_{qm}(\mathbf{r})=\sum_l U^F_{ql}F_{lm}(\mathbf{r}) , \tag{3.12}$$

with

$$U^F_{ql}=U^{F=0}_{ql}\times\begin{cases}A_+ \text{ for } l+m \text{ even}\\ A_- \text{ for } l+m \text{ odd} .\end{cases} \tag{3.13}$$

The presence of the factors $A_\pm$ makes U^F a nonorthogonal transformation. By combining (3.5), (3.8), (3.11a), and (3.13), the only coefficient that is relevant to later sections can be summarized as

$$U^F_{q0}=\pi^{1/2}(4/F)^{1/6}\mathcal{A}[-q^2/(2F)^{2/3}]\begin{cases}k^{-1/2} \text{ for } \varepsilon>0\\ \kappa^{-1/2} \text{ for } \varepsilon<0 .\end{cases} \tag{3.14}$$

Further, the $l=0$ wave function in (3.1) can be written as

$$F_{00}(\mathbf{r})=\int_{-\infty}^{k^2/2} d(q^2/2)[(U^F)^{-1}]_{0q}\psi^F_{q0}(\mathbf{r}) . \tag{3.15}$$

Although this formal inversion of (3.12) involves the inverse matrix U^{-1}, we will see that its explicit construction will be unnecessary, all our computations being functions of (3.14) alone.

C. Transformation for irregular functions

The wave function in (2.22) for the collision eigenchannels requires both the regular function f and the companion irregular function g. We need, therefore, a similar recasting of the irregular spherical functions $G_{lm}(\mathbf{r})$ in terms of the irregular cylindrical functions $\chi^F_{qm}(\mathbf{r})$. In the main the equality of Wronskians of pairs of solutions in the two symmetries allows us to write as the conjugate to (3.12)

$$\chi^F_{qm}(\mathbf{r})=\sum_l [(U^F)^{-1}]_{lq}G_{lm}(\mathbf{r}) , \tag{3.16}$$

along with the inverse relationship

$$G_{lm}(\mathbf{r})=\int_{-\infty}^{k^2/2} d(q^2/2)U^F_{ql}\chi^F_{qm}(\mathbf{r}) . \tag{3.17}$$

A subtle approximation is implicit in writing these expressions because, in common with the usual ambiguity in defining irregular functions,[17] these expressions can involve additive pieces proportional to the regular solutions (this will change neither the irregular behavior at the origin nor the Wronskian). Stated differently, when tunneling through an intervening barrier is involved, a pair of conjugate regular and irregular functions defined, say, at small r will in general upon continuation through the barrier not emerge at large r with the proper 90° out-of-phase relation between their oscillations. The amount by which the phase difference differs from 90° is represented by the coefficient of the additive pieces in (3.16) and (3.17) that involve the regular solutions. This coefficient, called cosecγ by Harmin,[5] and analogous to the quantum defect parameter $\mathcal{G}$,[7] is quite important in photoionization problems where there are many (infinite number) bound states and a substantial inner well. In our problem, however, where most negative ions have no more than one bound state (and that too with low binding energy), and the inner-well region is limited and small, we will ignore this complication. What this amounts to is that our matching of $F\neq 0$ and $F=0$ solutions as in (3.10), even though carried out at small distances, lies nevertheless already outside the barrier, the electron having tunneled out through the Fz barrier (clearly all this is only relevant to $q^2<0$). The $F\neq 0$ regular solution in (3.9) and the conjugate irregular one involving the irregular Airy function, which oscillate 90° out of phase at $z\to-\infty$ are still in the matching region similarly 90° out of phase, as are the cosqz and sinqz functions to which they are matched.

With (3.15) and (3.17) now in hand, we can rewrite ψ_ρ in (2.22) in terms of the cylindrical functions,

$$\psi_\rho=\sum_i T_{i\rho}\left[\cos\delta_\rho\int_{-\infty}^{k_i^2/2} d(q^2/2)\psi^F_{q0}[(U^F)^{-1}]_{0q} -\sin\delta_\rho\int_{-\infty}^{k_i^2/2} d(q^2/2)\chi^F_{q0}U^F_{q0}\right] . \tag{3.18}$$

Calculation of $D_{\rho\rho'}=\langle\Psi_\rho\,|\,\Psi_{\rho'}\rangle^{-1}$ leads to the same form given in Ref. 6,

$$\langle\psi_\rho\,|\,\psi_{\rho'}\rangle=\sum_i[\cos\delta_\rho\tilde{T}_{\rho i}(H^F_i)^{-1}T_{i\rho'}\cos\delta_{\rho'} +\sin\delta_\rho\tilde{T}_{\rho i}H^F_iT_{i\rho'}\sin\delta_{\rho'}] , \tag{3.19}$$

with

$$H^F(k)=\int_{-\infty}^{k^2/2} d(q^2/2)(U^F_{q0})^2 . \tag{3.20}$$

The modulating factor H^F, depending then only on U^F, encapsulates the entire effect of the external field. Although intermediate steps in the analysis involve the matrix U^{-1}, it could have been anticipated from the structure of (3.15) and (3.17) that, since physical significance is attributed only to the ratio of the coefficient of irregular to that of the regular function in a collision wave function (it is for this reason that tanδ or the K matrix are the objects of interest), such a ratio will involve the ratio of U to U^{-1}, that is, U^2. Therefore, H^F can be computed from only the single element U^F_{ql} with $l=0$. Analytical expressions of H^F for limiting values of energy and field strength are provided in Appendix C; in particular $H^F\to 1$ for $F\to 0$ as expected.

IV. PHOTODETACHMENT CROSS SECTIONS

The field dependence of the cross section is isolated in the density-of-states matrix $D^F_{\rho\rho'}$,

$$\sigma^F=\frac{4\pi^2\omega}{3(137)(2J_0+1)}\sum_J\sum_{\rho\rho'}d^J_\rho D^F_{\rho\rho'}d^J_{\rho'} . \tag{4.1}$$

The relevant zero-field reduced dipole matrix element involved is

$$d^J_\rho=\langle\psi^J_\rho\|r^{(1)}\|\Psi_0\rangle . \tag{4.2}$$

The dependence of the density-of-states matrix on J has been suppressed for notational brevity in (4.1). Here we treat the final continuum state of the negative ion in jj coupling, and make use of the Wigner-Eckart theorem to sum over magnetic quantum numbers analytically. This is permitted because the detachment cross section is independent of the incident light polarization, a consequence both of the negligible effect of the field on the atomic ground state and of the strong dominance of s waves in the photoelectron wave function.[18]

The number of relevant collision eigenchannels ψ_ρ^J depends on both J and the final-state energy E. For incident photon wave numbers in the range 16 755–17 152 cm^{-1}, only the $j=2$ channel is open. The relevant J values are then $\frac{3}{2}$ and $\frac{5}{2}$, with the latter giving no appreciable contribution to the photodetachment cross section because of spin conservation within region I. As discussed in Sec. II, the upper $j=1$ channel must be eliminated to give a single collision eigenchannel whose eigen-phase-shift $\delta_\rho^{(J=3/2)}$ is given by (2.13), thus determining a 1×1 density-of-states matrix,

$$D_{\rho\rho}^F = H^F(k_2)/\{\cos^2\delta_\rho^{(3/2)} + [H^F(k_2)\sin\delta^{(3/2)}]^2\} \ . \tag{4.3}$$

The eigenchannel dipole matrix element to be used in (4.1) involves only an $S=\frac{1}{2}$ region I reduced matrix element d^0 which can be regarded as a constant over the whole energy range considered in this paper,

$$d_\rho^J = c\,[U_{2,1/2}^{(3/2)} k_2^{1/2} + (c_1/c_2)(-i\kappa_1)^{1/2} U_{1,1/2}^{(3/2)}]d^0 \ , \tag{4.4}$$

with c as in (2.14) and c_1/c_2 as in (2.11a). Note that because of the dependence on $k_1=-i\kappa_1$ through K_{12}, the ratio c_1/c_2 carries a compensating $i^{-1/2}$ factor and the second term above is also explicitly real. We have finally in this energy range from (4.1)–(4.4),

$$\sigma^F = \sigma^{F=0} D_{\rho\rho}^F \ , \tag{4.5}$$

where the field-free cross section is the same as in Ref. 10,

$$\sigma^{F=0} = \frac{5}{6}\left[\frac{4\pi^2\omega}{137}\right](d^0)^2 \frac{k_2(1-\kappa_1 a_q)^2}{[1-\kappa_1(a_d+5a_q)/6]^2 + k_2^2[-\kappa_1 a_d a_q + (5a_d+a_q)/6]^2} \ . \tag{4.6}$$

The eigen-phase-shift required in these formulas is given explicitly by

$$\tan\delta_\rho^{(3/2)} = k_2[-\kappa_1 a_d a_q + (5a_d+a_q)/6]/[1-\kappa_1(a_d+5a_q)/6] \ . \tag{4.7}$$

Next, in the range 17 152–17 329 cm^{-1} photon energy, both channels $j=2$ and $j=1$ are open. Two values of the total angular momentum are now relevant, $J=\frac{3}{2}$ and $J=\frac{1}{2}$. For the $J=\frac{3}{2}$ contribution, the final state has both $j=1$ and $j=2$ channels present and open, and described by the two-channel reaction matrix (2.7). Since neither of these channels is closed, neither requires "elimination" in the quantum-defect-theory (QDT) sense. The two collision eigenchannel phase shifts $\delta_\rho^{(3/2)}$ and reduced dipole matrix elements $d_\rho^{(3/2)}$ are found by diagonalizing the matrix (2.7). More specifically, the two eigenvalues of $K_{jj'}^{(J)}$ are just $\tan\delta_\rho^{(J=3/2)}$, and the corresponding eigenvectors are just the $T_{j\rho}$ of Eq. (2.17) needed to determine the density-of-states matrix (3.19). If we denote these two $\tan\delta_\rho^{(J=3/2)}$ by λ_ρ, they are the roots of

$$\begin{aligned} &\lambda^2 + (A+B)\lambda + k_1 k_2 a_d a_q = 0 \ , \\ &A \equiv k_2(5a_d+a_q)/6, \quad B \equiv k_1(a_d+5a_q)/6 \ . \end{aligned} \tag{4.8}$$

The $J=\frac{3}{2}$ density-of-states matrix is

$$D_{\rho\rho'}^F = (ab-d^2)^{-1}\begin{vmatrix} b & d \\ d & a \end{vmatrix} \ , \tag{4.9a}$$

where we have defined

$$\begin{aligned} a &\equiv \frac{H^F(k_1)(\lambda_1+B)[1+\lambda_1^2 H^F(k_2)^2] + H^F(k_2)(\lambda_1+A)[1+\lambda_1^2 H^F(k_1)^2]}{H^F(k_1)H^F(k_2)(1+\lambda_1^2)(\lambda_1-\lambda_2)} \ , \\ b &\equiv a \quad \text{with } \lambda_1 \leftrightarrow \lambda_2 \ , \\ d &\equiv \left[\frac{(\lambda_1+A)(\lambda_1+B)}{(1+\lambda_1^2)(1+\lambda_2^2)}\right]^{1/2}\left[\frac{1+\lambda_1\lambda_2 H^F(k_1)^2}{H^F(k_1)} - \frac{1+\lambda_1\lambda_2 H^F(k_2)^2}{H^F(k_2)}\right]\frac{1}{\lambda_1-\lambda_2} \ , \end{aligned} \tag{4.9b}$$

when $F=0$, $H^F=1$ and $D_{\rho\rho'}^F$ reduces to the unit matrix as it should. The reduced dipole matrix elements again pick out only the $S=\frac{1}{2}$ contribution as in (4.4), giving explicitly

$$d_\rho^{(J)} = d^0 \sum_j k_j^{1/2} U_{j,S=1/2}^{(J)} T_{j\rho} \ . \tag{4.10}$$

The $J=\frac{1}{2}$ part of the photodetachment cross section involves now the two channels $j=1$ and $j=0$, of which the latter must be eliminated since it is a closed channel. The resulting formula for the lone collision eigen-phase-shift $\delta_\rho^{(J=1/2)}$ is then obtained from (2.15), and the contribution to the cross section from $J=\frac{1}{2}$ is

$$\sigma^F(J=\tfrac{1}{2})=\sigma^{F=0}(J=\tfrac{1}{2})H^F(k_1)/\{\cos^2\delta_\rho^{(1/2)}+[H^F(k_1)\sin\delta_\rho^{(1/2)}]^2\}\ , \tag{4.11}$$

with

$$\sigma^{F=0}(J=\tfrac{1}{2})=\frac{2}{15}\frac{4\pi^2\omega}{137}(d^0)^2\frac{k_1(1-\kappa_0 a_q)^2}{[1-\kappa_0(a_d+2a_q)/3]^2+k_1^2[-\kappa_0 a_d a_q+(2a_d+a_q)/3]^2} \tag{4.12}$$

and

$$\tan\delta_\rho^{(1/2)}=k_1[-\kappa_0 a_d a_q+(2a_d+a_q)/3]/[1-\kappa_0(a_d+2a_q)/3]\ . \tag{4.13}$$

Finally, above 17 329 cm^{-1} all channels are open for photoabsorption from S^- in the $^2P_{3/2}$ ground state. Again two values of the angular momentum contribute, with $\sigma^F(J=\frac{3}{2})$ still given by the result derived in the previous paragraph. The $J=\frac{1}{2}$ part of the cross section involves a two-channel calculation closely analogous to that derived for $J=\frac{3}{2}$ in the previous paragraph and will not be given explicitly here. Transitions from the $^2P_{1/2}$ state of the negative ion to the $j=2$, 1, and 0 continuum channels are analyzed identically. The only numerical difference is in the short-range dipole matrix element d^0, a common factor in all the above cross-section formulas. This d^0 is now evaluated with the wave function appropriate to the $^2P_{1/2}$ state of S^-. The resulting change in the numerical values is as in Ref. 10.

All expressions for the cross section σ^F close to a threshold j show a term proportional to $H^F(k_j)$. Examination of the proportionality constant in the vicinity of threshold, $k_j\simeq 0$, shows [see (C3)] a $1/k_j$ behavior. This cancels the dependence on k_j (Wigner threshold law) contained in this portion of σ^F so that the field-dependent cross section σ^F starts at a finite value at each threshold. For instance at the lowest threshold j for a given J,

$$\sigma^F(J;k_j=0)=(\tfrac{3}{32})^{1/3}\Gamma^2(\tfrac{2}{3})(F^{1/3}/\pi)\times[\sigma^{F=0}(J)/k_j]_{k_j=0}\ . \tag{4.14}$$

Note the proportionality to $F^{1/3}$. The same limiting value of σ^F applies when the threshold is approached from below. Therefore, unlike in the $F=0$ case, the cross sections now go smoothly through each threshold. Far below threshold, the expression (C6) for $H^F(\kappa_j)$ shows a rapidly falling exponential dependence on κ^3/F. This arises as expected from the tunneling through the barrier formed by the electric field. In fact, (C6) is essentially the well-known expression for the field-ionization cross section, when writing it as

$$(\pi F/\kappa)\left[\frac{1}{2\pi\kappa^2}\right]\exp(-2\kappa^3/3F)\ , \tag{4.15}$$

where the second term in parentheses expresses our normalization per unit energy. Standard textbooks[12] quote a result which has instead of this factor the factor $(2\pi)^{-1}$ that is relevant to normalization to unit current density of the outgoing field-ionized electrons.

V. RESULTS AND SUMMARY

The key quantity for photodetachment in an electric field is the modulating factor H^F in (3.20). Figures 1 and 2 show a plot of this function as a function of the energy for two representative values of the field strength, $F=10^{-5}$ and 5×10^{-5} a.u. (5×10^4 and 2.5×10^5 V/cm). H^F is a continuous function from $-\infty$ to ∞. For negative energies, the tunneling region, there is a rapid falloff. At positive energies, the function oscillates, with damped oscillations dying down to the asymptotic value of unity. The spike at $k=0$ represents the contribution from (C3), with its $1/k$ and $1/\kappa$ structure on either side of this limit.

Figure 3 shows the cross section for photodetachment from the $^2P_{3/2}$ state of S^- (likewise, Fig. 4 for detachment from the $^2P_{1/2}$ state) for the two field strengths. In comparison to the $F=0$ cross section, shown by dashed lines, note the modulations superimposed by the factor H^F. The characteristic "square-root" dependence on the energy of the $F=0$ results at the threshold are also absent now in σ^F. In gathering together the expressions for σ_j^F derived in Sec. IV, we have used $a_d=3.5$ a.u. and $a_q=-10$ a.u., values drawn from Ref. 10. Note that just as in that analysis of field-free photodetachment, these two parameters that characterize the short-range interaction of the electron with the S atom (and, therefore, they remain the same for $F=0$ and $F\neq 0$) are the only ones

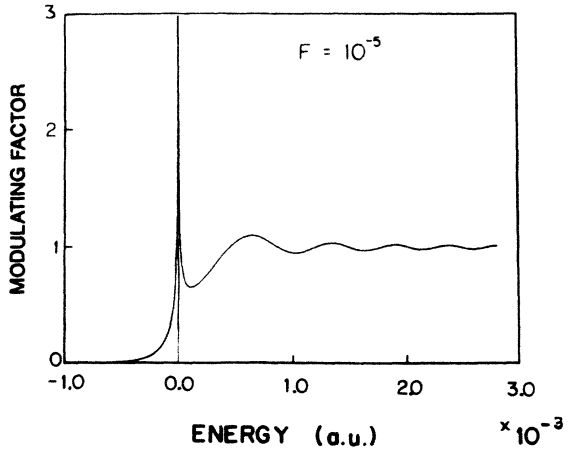

FIG. 1. Modulating factor H^F in Eq. (3.20) for a field of $F=10^{-5}$ a.u.

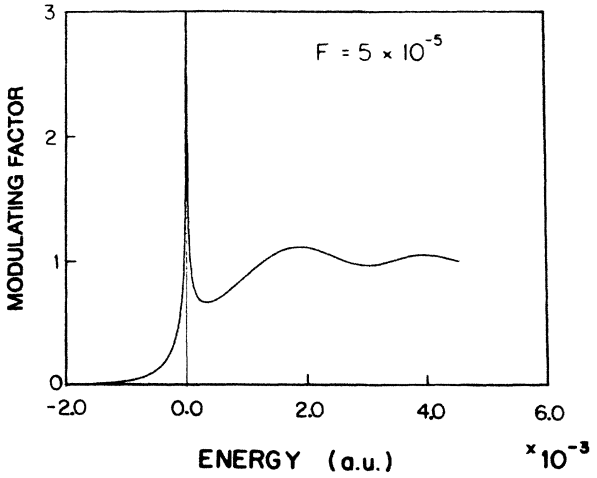

FIG. 2. Same as Fig. 1 for $F = 5 \times 10^{-5}$ a.u.

not determined by our analysis. Everything else is handled as a series of frame transformations and the dependences worked out analytically.

The presence of the electric field F is thus seen in Figs. 3 and 4 to overturn the square-root threshold singularities observed at each fine-structure threshold in zero field. The cross section is now finite and smooth near each such threshold. In more physical terms, the field-induced modulations can be regarded as an interference between two paths leading to photoelectron escape. For the first path the photoelectron moves "downstream" from the atom toward $z = -\infty$ immediately after the photoabsorption. For the second path the photoelectron initially heads "upstream," moving to $z \sim F/E$ before being reflected backward and escaping to $z = -\infty$. Fabrikant[19] has shown that this interpretation can be combined with

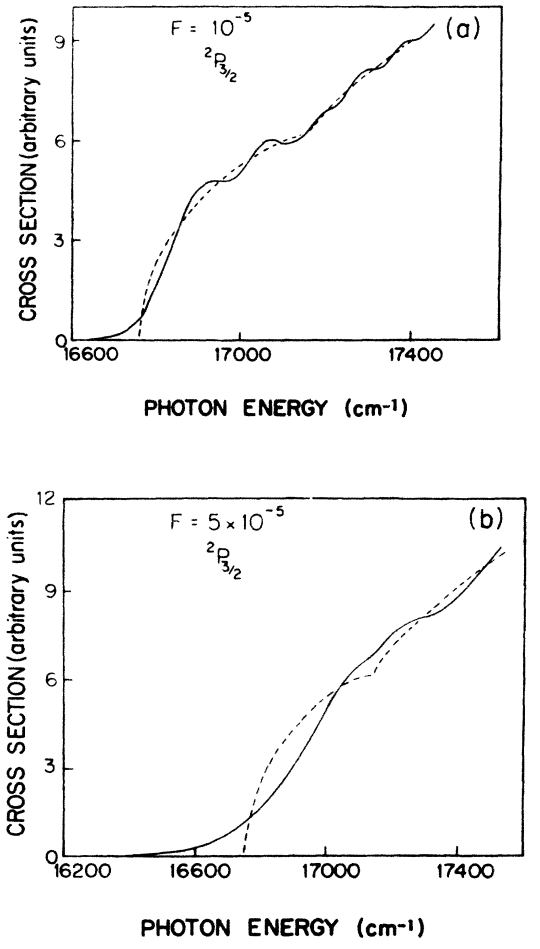

FIG. 3. Photodetachment cross-section from the $^2P_{3/2}$ state of S^- in fields of (a) 10^{-5} a.u. (b) 5×10^{-5} a.u. Dashed lines indicate the zero-field cross section. The incident radiation is polarized linearly along the field axis.

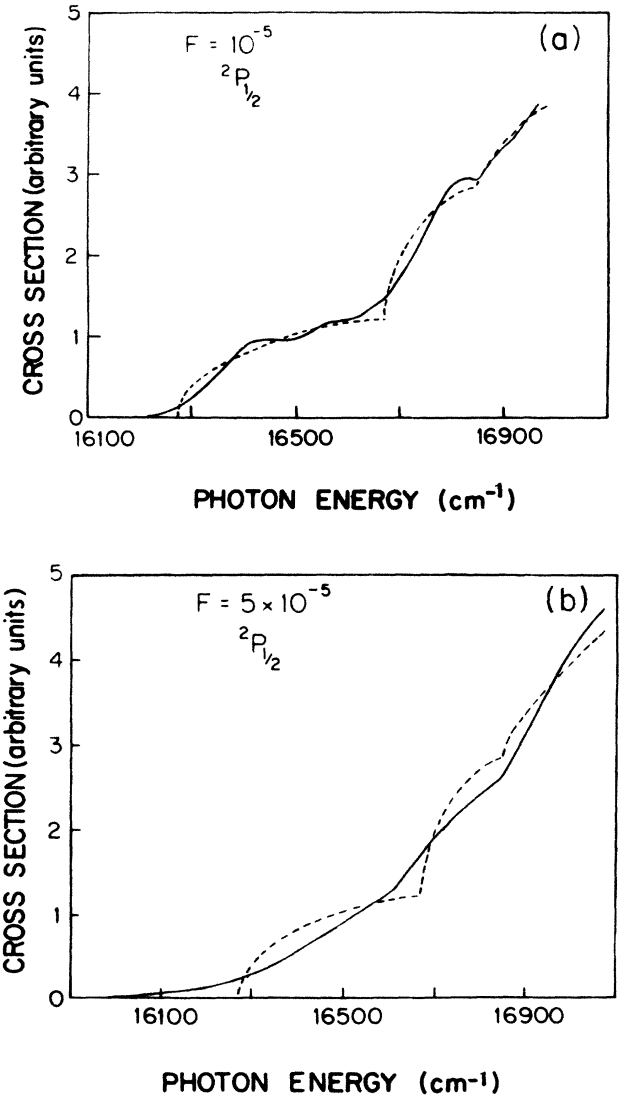

FIG. 4. Same as Fig. 3 but for the $^2P_{1/2}$ state.

a semiclassical analysis to predict that the nth maximum of these interference oscillations occurs at an energy $E_n=(0.067Fn)^{2/3}$ cm^{-1}, where F is the electric field in V/cm. (This result neglects the electron-atom interaction altogether, in contrast to our frame transformation analysis.)

Bryant *et al.*[4] have recently observed these field-induced modulations, as well as detachment *below* the zero-field threshold (caused by tunneling), in H^- photodetachment. The theoretical treatment developed in this paper applies to H^- photodetachment, with a few modifications associated with the fact that the photoelectron escapes with $l=1$ rather than $l=0$. Another paper[22] shows that this analysis accounts for the experimental spectrum of Ref. 4 quantitatively.

ACKNOWLEDGMENT

This work has been supported by the National Science Foundation under Grants No. PHY-86-07721 and No. PHY-87-40404.

APPENDIX A: ALTERNATIVE NORMALIZATIONS AT SMALL r

Our use of radial functions in Sec. II for regions I and II has followed the now-standard form for the quantum-defect theory of functions (2.1) defined independent of the energy in region I and normalized per unit energy scale in region II, as in (2.5). This choice also conforms to the one adopted in Ref. 10 for the zero-field photodetachment of S^-. With this choice, the functions (2.5) upon examination in the $r\to 0$ limit display energy-dependent factors, $k_j^{\pm 1/2}$. An alternative procedure, used in the companion paper,[6] is to use functions wherein these factors have been filtered out so that critical energy dependences do not appear at the step of matching (2.5) to (2.1). [As noted in (2.2), the same goal can also be attained by modifying suitably the functions in (2.1).] In the main, for our problem, this removes some of the factors k_j in some of the expressions in the text, to reappear elsewhere.[23] We catalog these changes here.

Replacing (2.5) and its counterpart (3.6) at negative energies by

$$f^0(r)=\begin{cases}(2/\pi)^{1/2}k^{-1}\sin kr, & g^0(r)=-(2/\pi)^{1/2}\cos kr, \quad \varepsilon>0\\ (2/\pi)^{1/2}\kappa^{-1}\sinh\kappa r, & =-(2/\pi)^{1/2}\cosh\kappa r, \quad \varepsilon<0\end{cases} \tag{A1}$$

the reaction matrix in (2.7) is now smooth and analytic at $\varepsilon=0$,

$$K_{jj'}^{(J)0}=-\sum_S U_{jS}^{(J)}a_S U_{j'S}^{(J)} . \tag{A2}$$

A wave function, such as in (2.12) takes the form

$$\psi^0=c^0\phi(f^-g^0\tan\delta^0) , \tag{A3}$$

where the analog of (2.14) still applies;

$$c^0=(1+\tan^2\delta^0)^{-1/2} , \tag{A4a}$$

and

$$\tan\delta^0=k^{-1}\tan\delta . \tag{A4b}$$

Similar changes occur elsewhere in Sec. II.

Turning to Sec. III, the definitions in (A1) now lead in place of (3.8) to

$$U_{q0}^{0,F=0}=q^{-1/2} , \tag{A5}$$

so that in (3.20)

$$H^F(k)^0=kH^F(k) . \tag{A6}$$

Likewise, the cross-section expressions in Sec. IV are modified;

$$\sigma^F=\frac{4\pi^2\omega}{3(137)(2J_0+1)}\sum_J\sum_{\rho\rho'}d_\rho^J D_{\rho\rho'}^0 d_{\rho'}^J \tag{A7}$$

replaces (4.1), where D^0 is evaluated from (4.2) or (4.9) after using (A4b) and (A6) to replace quantities by their superscript-zero counterparts. The final expressions and numerical results of Secs. IV and V are, of course, unchanged.

APPENDIX B: EVALUATION OF THE TRANSFORMATION MATRIX $U_{ql}^{F=0}$

The key element of Sec. III is the transformation from spherical to cylindrical symmetry. Once established for $F=0$ we saw how it is readily adapted to the form relevant for $F\neq 0$. The first part of this result, namely $U_{ql}^{F=0}$ in (3.4), was obtained in Sec. III for $l=0$ very simply by inspection of the small distance behavior of the wave functions. Here we will consider alternative routes to this results and some generalizations.

Considering $l=0$ first, the right-hand side of (3.1) is explicitly independent of angles, leading to

$$U_{q0}^{F=0}F_{00}(\mathbf{r})=\int_0^{\pi/2}d\theta\sin\theta J_0[(k^2-q^2)^{1/2}r\sin\theta] \times(\pi q)^{-1/2}\cos(qr\cos\theta) . \tag{B1}$$

Evaluating the integral, we have

$$U_{q0}^{F=0}F_{00}(\mathbf{r})=(2q)^{-1/2}(kr)^{-1/2}J_{1/2}(kr) ; \tag{B2}$$

that is,

$$F_{00}(\mathbf{r})=\int_0^{k^2/2}d(q^2/2)\psi_{q0}(\mathbf{r})U_{q0}^{F=0} , \tag{B3}$$

which is the inverse of (3.4).

Finally, although unnecessary for our purposes in the paper, note that more generally for any l, we can write from (3.4) upon using the orthonormality of the angular functions contained in (3.1),

$$U_{ql}^{F=0} r^{1/2} J_{l+1/2}(kr) = N_{lm}(\pi q)^{1/2} \int_0^{\pi} d\theta \sin\theta J_m[(k^2-q^2)^{1/2}\rho] \times P_l^m(\cos\theta) \times \begin{cases} \cos qz \\ \sin qz \end{cases} . \quad \text{(B4)}$$

The integral on the right-hand side can be worked out in closed form for special values of m. For example, for $m=l$, when $P_l^m \sim \sin^l\theta$, the integral is proportional[21] to $J_{l+1/2}(kr)$, so that matching coefficients on both sides of (B4) gives

$$U_{ql}^{F=0} = (-i)^l[(2l+1)/(2l)!]^{1/2}(kq)^{-1/2} P_l^l(q/k), \quad m=l . \quad \text{(B5)}$$

APPENDIX C: EVALUATION OF THE MODULATING FACTOR H^F

In the final expressions for detachment cross sections in an electric field, the modulating factor encapsulates the entire influence of the field. We will derive here expressions in various limits for this factor. As given in (3.20), with U^F taken from (3.14), we have for $\varepsilon > 0$

$$H^F(k) = (4/F)^{1/3}(\pi/k) \int_{-\infty}^{k^2/2} \mathcal{A}[-q^2/(2F)^{2/3}] d(q^2/2) . \quad \text{(C1)}$$

It is useful to split the range of integration into two pieces, and rewrite as

$$H^F(k) = (4/F)^{1/3}(\pi/k) \times \left[\int_0^{\infty} d(q^2/2) \mathcal{A}^2[q^2/(2F)^{2/3}] + \int_0^{k^2/2} d(q^2/2) \mathcal{A}^2[-q^2/(2F)^{2/3}] \right] . \quad \text{(C2)}$$

Note immediately that as $k \to 0$ only the first term survives and will be proportional to $1/k$. In fact, the integral involved can be worked out analytically and we have

$$H^F(k \to 0) = (\tfrac{3}{32})^{1/3} F^{1/3} \Gamma^2(\tfrac{2}{3})/\pi k . \quad \text{(C3)}$$

The second term in (C2) can be evaluated numerically for some value of k. When $F \to 0$, it is this term that dominates because, as follows from (C3), the first term in (C2) vanishes in this limit. In this limit, the second term and therefore $H^F(k)$ can be shown to reduce to unity as follows. For the Airy function with large negative argument, write[22] $\mathcal{A}^2(-x) = (1/\pi)x^{-1/2}\sin^2(2x^{3/2}/3 + \pi/4)$ and replace the rapidly oscillating $\sin^2$ function in the integrand by its average value of $\frac{1}{2}$ to get

$$(2F)^{1/3}(2k)^{-1} \int_0^{k^2/(2F)^{2/3}} dx\, x^{-1/2} ,$$

which reduces to unity.

Below the threshold, we have from (3.20) and (3.14),

$$H^F(\kappa) = (4/F)^{1/3}(\pi/\kappa) \times \int_{-\infty}^{-\kappa^2/2} d(q^2/2) \mathcal{A}^2[-q^2/(2F)^{2/3}] . \quad \text{(C4)}$$

Once again, clearly as $\kappa \to 0$, this reduces to (C3) except that k is replaced by κ. On the other hand, for κ large, that is, far below threshold, the Airy function of large positive argument can be approximated[23] by $\mathcal{A}^2(x) = (4\pi)^{-1}x^{-1/2}\exp(-4x^{3/2}/3)$ so that (C4) takes the form

$$H^F(\kappa \gg 1) = F^{1/3}(12)^{-2/3} \int_{2\kappa^3/3F}^{\infty} e^{-u} u^{-2/3} du . \quad \text{(C5)}$$

The integral is proportional[24] to the Whittaker function $W_{-1/3,1/6}(2\kappa^3/3F)$ whose known asymptotic properties give finally

$$H^F(\kappa \gg 1) = (F/4\kappa^3)\exp(-2\kappa^3/3F) . \quad \text{(C6)}$$

[1] See, for instance, several papers in *Atomic Excitation and Recombination in External Fields*, edited by M. H. Nayfeh and C. W. Clark (Gordon and Breach, New York, 1985).

[2] See a review, D. Kleppner, M. G. Littman, and M. L. Zimmerman, in *Rydberg States of Atoms and Molecules*, edited by R. F. Stebbings and F. B. Dunning (Cambridge University Press, Cambridge, England, 1983), p. 73.

[3] W. A. M. Blumberg, R. M. Jopson, and D. J. Larson, Phys. Rev. Lett. **40**, 1320 (1978).

[4] Very recently, results have been reported on photodetachment of H^- in an electric field, H. C. Bryant *et al.*, Phys. Rev. Lett. **58**, 2412 (1987).

[5] D. A. Harmin, Phys. Rev. A **26**, 2656 (1982); K. Sakimoto, J. Phys. B **19**, 3011 (1986).

[6] C. H. Greene, Phys. Rev. A **36**, 4236 (1987).

[7] U. Fano and A. R. P. Rau, *Atomic Collisions and Spectra* (Academic, Orlando, 1986), pp. 158 and 159.

[8] U. Fano, Phys. Rev. A **24**, 619 (1981).

[9] L. D. Landau and E. M. Lifshitz, *Quantum Mechanics, Non-Relativistic Theory*, 3rd ed. (Pergamon, Oxford, 1977), Sec. 77.

[10] A. R. P. Rau and U. Fano, Phys. Rev. A **4**, 1751 (1971).

[11] W. C. Lineberger and B. W. Woodward, Phys. Rev. Lett. **25**, 424 (1970).

[12] Ref. 9, p. 294.

[13] Ref. 7, Sec. 4.3.2; Ref. 9, Secs. 21 and 33.

[14] U. Fano and G. Racah, *Irreducible Tensorial Sets* (Academic, New York, 1969), Eq. 13-14; see also Ref. 7.

[15] Ref. 7, Secs. 7.4.4 and 8.6.1.

[16] M. Abramowitz and I. A. Stegun, *Handbook of Mathematical Functions* (Dover, New York, 1972), Sec. 10.4.

[17] Ref. 7, Sec. 5.11.

[18] This choice has been made for simplicity. More generally, if the direction of propagation of the photon is at an arbitrary angle with respect to the electric field, a mixture of different M_J values will contribute to the final state.

[19] I. I. Fabrikant, Zh. Eksp. Teor. Fiz. **79**, 2070 (1980) [Sov. Phys.—JETP **52**, 1045 (1980)].

[20] A. R. P. Rau and Hin-Yiu Wong, Phys. Rev. A **37**, 632 (1988).

[21] I. S. Gradshteyn and I. M. Ryzhik, *Table of Integrals, Series and Products* (Academic, New York, 1980), Eq. 6.688.2.

[22] Ref. 16, Eq. 10.4.60.

[23] Ref. 16, Eq. 10.4.59.

[24] Ref. 21, Eq. 3.381.6.